BES Analysis Memo
Observation of $\psi(2S)$ Radiative Decays

Li Xinhua
email: LIXH@bepc5.ihep.ac.cn

Abstract

A sample of 3.6×10^6 produced $\psi(2S)$ events collected by BES detector at BEPC is used to investigate the radiative decays of $\psi(2S)$ to non-charmonium states. Significant f_2 and η' signals have been observed in addition to an initial state radiation production of ρ^0 via QED process. The related branching fractions have been obtained and compared with the expectation of perturbative QCD. While γf_2 obeys the prediction, $\gamma\eta'$ is suppressed by a factor of 4. There currently exists no compelling explanation for the discrepancy between the ratio measured for these decays and theoretical expectation.

Key words $\psi(2S)$ **radiative decay, branching fraction, abnormal suppression.**

The $\psi(2S)$ decay is conventionally compared with the corresponding J/ψ decay to understand the nature of $c\bar{c}$ annihilation. In lowest order of perturbative QCD[1], the partial width of the J/ψ or $\psi(2S)$ to three gluons is proportinal to the square of the wavefunction at the origin, as is the partial width to leptons. If the hadronization of the gluons is not substantially different at the mass of $\psi(2S)$ from at the mass of J/ψ, one obtains a universal ratio

$$\frac{B(\psi(2S) \to X)}{B(J/\psi \to X)} = \frac{B(\psi(2S) \to ggg)}{B(J/\psi \to ggg)} = \frac{B(\psi(2S) \to e^+e^-)}{B(J/\psi \to e^+e^-)} = 0.147 \pm 0.023.$$

where X is an arbitrary non-charmonium state and the PDG[2] data are adopted for lepton pair decay.

Mark II collaboration has systematically investigated hadronic decays of $\psi(2S)$ and found most channels observe the theoretical expectation with absence of vector-pseudoscalar combinations, $\rho\pi$ and K^*K[3]. Over years, theoretic attepts have been taken without compelling explanation for the discrepancy between the ratios measured for the decays and theoretical expectation. Recently BES collaboration has observed that the hadronic decay of $\psi(2S)$ into vector-tensor combinations, ωf_2, ρa_2 and $K^{*0}K_2^{*0}$, are suppressed at a level of 5 or even larger[4, 5].

The status of radiative decay is not clear because only a few of large upper limits arise in PDG for the non-charmonium decay of $\psi(2S)$. The lowest order

expression of the partial width of J/ψ or $\psi(2S)$ decay to a photon and two gluons also depends on the square of the wavefunction at the origin[6]. Thus one expects the "15% $rule$" stands also for radiative decays of $\psi(2S)$ and J/ψ to any non-charmonium hadron. This paper dedict to investigate the radiative decay of $\psi(2S)$ to non-charmonium states. Specifically, we measure the branching fractions of the reactions $\psi(2S) \rightarrow \gamma f_2$ and $\gamma\eta'$ with standard exclusive analyses via final states consisting of one or two photon and a pair of charged tracks.

The BES detector has been detailed in [7]. Here we briefly describle detector elements crucial to this measurement. Tracking is provided by a 10 superlayer main drift chamber (MDC). Each superlayer contains four layers of sense wires measuring both the position and the ionization energy loss (dE/dx) of charged particles. The momentum resolution is $\sigma_P/P = 1.7\%\sqrt{1+P^2}$, where P is the momentum in GeV/c. The resolution of dE/dx measurement is 11% for hadron tracks. This provides good π/K separation and proton identification in low momentum region. An array of 48 scintillation counters surrounds MDC which measures the time-of-flight (TOF) of charged tracks with a resolution of 450 ps for hadrons. Outside the TOF system is an electromagnetic calorimeter composed of streamer tubes and lead blocks with a z positional resolution of 4 cm. The energy resolution scales as $\sigma_E/E = 0.22/\sqrt{E}$, where E is the energy in GeV. Surrounding the shower counter is a solenoidal magnet providing a 0.4 Tesla magnetic field in the central tracking region of the detector. The muon detector system lies outside the magnetic field and is used to measure the coordinates of muons in z and in $r\phi$ with resolution 5 cm and 3 cm, respectively. The analysis is based on a sample of 3.6×10^6 produced $\psi(2S)$ events collected by the Beijing Spectrometer detector at the Beijing Electron Positron Collider in 1995 running.

Events of two opposite charged tracks with transverse momenta above 70 MeV/c and vertex in the colliding zone have been selected. These two charged tracks are neither back-to-back within 5^o nor identified as electrons or muons. Charged pions are identified when track momenta are under 0.7 GeV/c by using dE/dx and TOF measurements. Photon signals are searched for in barrel shower counter with deposited energy larger than 60 MeV and no stand-by associated charged tracks. The angle between a photon entering shower counter and its cluster going through is required to be less than 20^o to exclude the coincidence of complicated noise. Corrections are made for energy loss and multiple Coulomb scattering by charged particles passing materials before they enter the drift volume in BES inner detector. So are photon directions entering shower counter for event vertex dispersions in the colliding zone.

Furthermore, kinematic cuts are made for specifical final states. Frankly are missing momentum $\vec{P}_{miss}$ and missing energy E_{miss} of charged tracks by using the pion mass hypothesis. Characteristic variables of radiative decay are $U_{miss} = E_{miss} - P_{miss}$ and $P_{tr}^2 = 4P_{miss}^2 \sin^2\theta_\gamma/2$, where θ_γ is the angle between photon and $\vec{P}_{miss}$. $P_{tr}^2 < 6400(MeV/c)^2$ and $\mid U_{miss} \mid < 0.2GeV$ are required to select only one photon final state. Events with at least one detected photon are kinematically $2C1\gamma$ fitted and the probabilities are required to be larger than 0.05

to improve the mass resolution and increase the ability to reject background. After above selection, contamination of J/ψ decays are almost free due to final state contaning only one hard photon.

The $\pi^+\pi^-$ mass spectrum, as shown in Fig. 1, indicates significant f_2 signal and also a lower mass structrure of ρ^0. The f_2 signal and ρ^0 signal have been fitted to Breit-Wigner curves with the corresponding width fixed to PDG added to a quadratic background. The combined fit leads to 151 ± 25 f_2 signal with mass $(1245 \pm 14)MeV$ and 157 ± 22 ρ^0 signal with mass $(743 \pm 10)MeV$.

The production of ρ^0 consists with a QED process - initial state radiation (ISR) of photon by the e^+ or e^-, followed by $e^+e^- \to$ vector meson[8]. This QED production has been observed for the first time by Crystal Ball Group at SPEAR[9]. The cross section of $\gamma\rho^0$ production is 1.2nb in e^+e^- annihilation at mass center energy 3.686 GeV[10]. The polar angle distribution of photon is approximately $\frac{1}{\sin^2\theta}$ for large angle in case of high momentum beam. Producing events with polar angle of photon larger than 35^o which is 13% of the whole range, Monte Carlo simulation gives analysis efficiency 3.6%. The integrated luminosity for the whole $\psi(2S)$ running is $6.2pb^{-1}$. One obtains

$$\sigma(e^+e^- \to \gamma\rho^0) = (0.71 \pm 0.10 \pm 0.19)nb$$

where the first error is statistic and second systematic which is dominanted by event analysis.

The analysis efficiency of γf_2 is 30.1% calculated by Monte Carlo simulation with uniform phase space distribution and combining detector status addition to data process. Adopting an isospin ratio 2:1 for f_2 decays into $\pi^+\pi^-$ or $\pi^0\pi^0$, one obtains

$$B(\psi(2S) \to \gamma f_2) = (2.46 \pm 0.41 \pm 0.67) \times 10^{-4}$$

where the first error is statistic and second systematic which mainly due to event analysis and Monte Carlo simulation.

η' is reconstructed via its decay to $\gamma\rho^0$ in $\gamma\gamma\pi^+\pi^-$ final state. Although γ_1 is monoenergy, γ_2 has low energy with wide distribution. This channel is complicated by even unknown backgrounds. Such as $\psi(2S)$ directly decay to $\rho^0\pi^0\pi^0$, J/ψ decay to $\rho\pi$, $\gamma\eta'$, γf_2 and so on via $\psi(2S)$ decay to neutrals and J/ψ. Instead of Umiss cut which is not effective because of the invariant mass of two photons with wide distribution, we require Pmiss¿1GeV/c. Moreover, we adopt $\theta_{\gamma\gamma} > 120^o$ with typical event topology. Both cuts lose respectively 3% efficiency checked by Monte Carlo simulation. The highest energy photon is taken as γ_1. Events with at least two detected photons are kinematically $2C2\gamma$ fitted and the probability is required to be larger than 0.05. γ_2 is selected corresponding to the highest probability. Figure 2(a) shows $\pi^+\pi^-$ mass spectrum which indicates ρ^0 signal. Selecting ρ^0 mass band within 650 and 880 MeV/c^2, $\gamma\rho^0$ mass plot is shown on figure 2(b) which shows η' signal.

Potential background dominates by $\psi(2S)$ decays to $n\gamma J/\psi$ via χ_c, η and π^0 decay with J/ψ decay to $n\gamma\pi^+\pi^-$ state including $\rho\pi$, $\gamma\eta'$, γf_2 etc. Direct decay of $\psi(2S)$, such as $\psi(2S) \to \rho^0\pi^0\pi^0$, may also contribute to background. Monte Carlo produces events expected from the $\psi(2S)$ number and PDG branching fractions of the above decay modes. Figure 3(b) shows the resulting $\gamma\rho^0$ mass plot. These background contaminations into data sample are not severe and contribute to almost flat spectrum. Gaussian fit with linear background gives η' mass $(961 \pm 3)MeV/c^2$ and mass resolution $(10.1 \pm 2.5)MeV/c^2$ and leads to event number 20.9 ± 5.4. The angular distribution is unique in the cascade decays $\psi(2S) \to \gamma_1\eta'$ with $\eta' \to \gamma_2\rho^0$ and $\rho^0 \to \pi^+\pi^-$ because of pseudoscalar meson η'

$$\frac{d^2\sigma}{d\cos\theta_{\gamma_1} d\cos\theta_{\pi^-}} = (1 + \cos^2\theta_{\gamma_1})\sin^2\theta_{\pi^-}.$$

Producing with these distributions, Monte Carlo simulation give analysis efficiency 13.3%. Adopting $B(\eta' \to \gamma\rho^0)$ of PDG value, one calculates the branching fraction

$$B(\psi(2S) \to \gamma\eta') = (1.45 \pm 0.37 \pm 0.36) \times 10^{-4},$$

where the first error is statistic and second systematic. This value is well under the upper limit of PDG, 1.1×10^{-3}, of this decay channel. Taking its branching ratio in J/ψ decay of PDG, one obtains the ratio

$$B(\psi(2S) \to \gamma\eta')/B(J/\psi \to \gamma\eta') = (3.4 \pm 1.2)\%$$

which is roughly a factor of six below the theoretically expectation in Eq. (2).

In summary, we observed f_2 and η' signal in radiative decays of $\psi(2S)$ in 3.6×10^6 data sample and even an initial state radiation production of ρ^0. The measured branching fractions are compared with the corresponding J/ψ decays. While the ratio of γf_2 is consistent with theoretical expectation of perturbative QCD, $\gamma\eta'$ is suppressed by at least a factor of 2. A lower mass structrure of ρ^0 is also observed in the final state $\gamma\pi^+\pi^-$. It consists with a QED process - initial-state radiation of photon by the e^+ or e^-, followed by $e^+e^- \to \rho^0$. The measured cross section, $(0.71 \pm 0.10 \pm 0.19)nb$, agrees with QED expectation.

REFERENCES

1. T.Applequist, D.Politzer, Phys. Rev. Lett. 34, 43(1975).
2. Particle Data Group, Phys. Rev., D50 part I (1994).
3. M.E.B.Franklin et al., Phys. Rev. Lett. 51, 11(1983).
4. BES Collaboration, High Energy Physics and Nuclear Physics (in Chinese), 19 (1995) 93.
5. Jin Li, Experimental Progress on Charmonium and Light Hadron Spectroscopy, XVII Inter. Symp. on Lepton - Photon Interactions, Beijing, August 10-15, 1995; BES Collaboration, contribution to this symposium.
6. W. Kwong, Phys. Rev., D37 (1988) 3210.
7. BES Collab., Nucl. Inst. Meth., A344 (1994) 319.
8. R.A.Lee, SLAC-PUB-3676, May 1985.
9. J.D. Jackson and D.L. Scharre, Nucl. Instru. Methods, 128, 13(1975); G.Bonneau and F.Martin, Nucl. Phys. B, 27, 381(1971).

TABLES

TABLE I. Results compared with J/ψ data of PDG

Mode	$B(\psi(2S))$	$B(J/\psi)$	$B(\psi(2S))/B(J/\psi)$
γf_2	$(2.46 \pm 0.41 \pm 0.67) \times 10^{-4}$	$(1.38 \pm 0.14) \times 10^{-3}$	$(17.8 \pm 6.0)\%$
$\gamma \eta'$	$(1.45 \pm 0.37 \pm 0.36) \times 10^{-4}$	$(4.31 \pm 0.30) \times 10^{-3}$	$(3.4 \pm 1.2)\%$

FIGURES

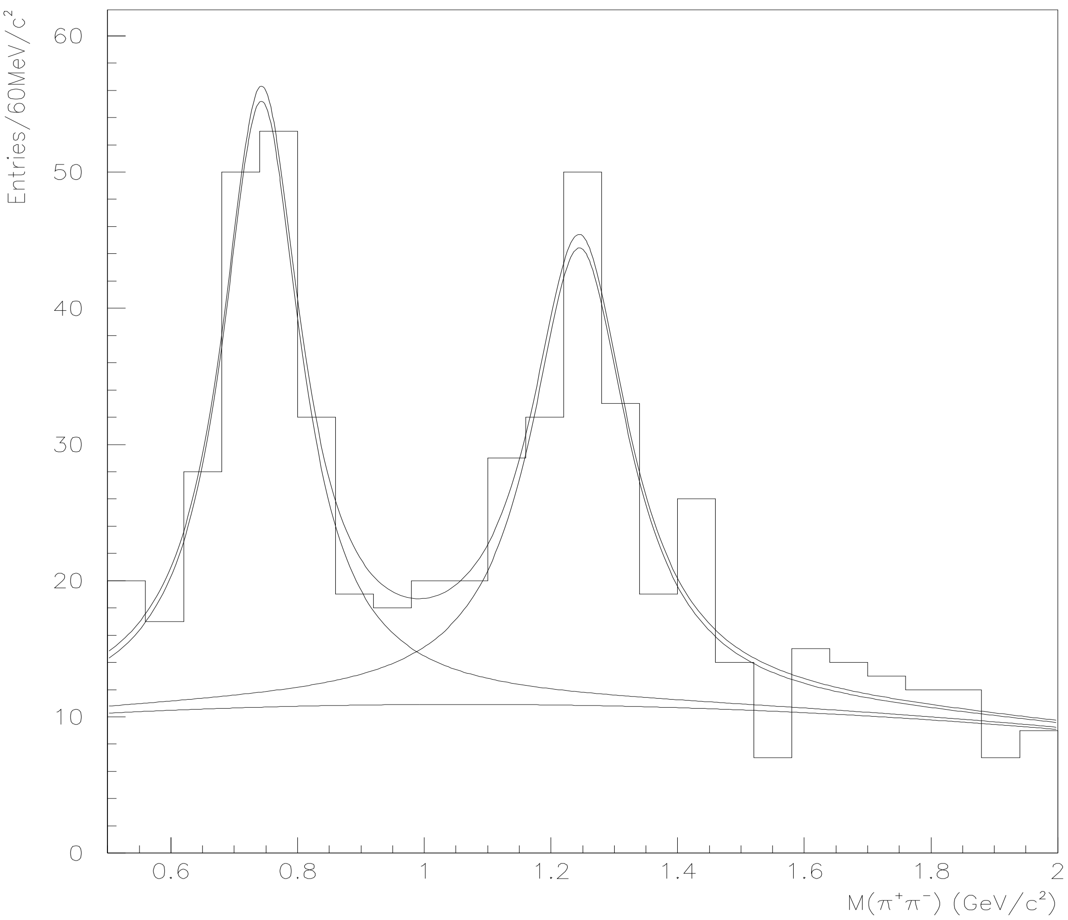

FIG. 1. $\pi^+\pi^-$ mass in $\gamma\pi^+\pi^-$ final state

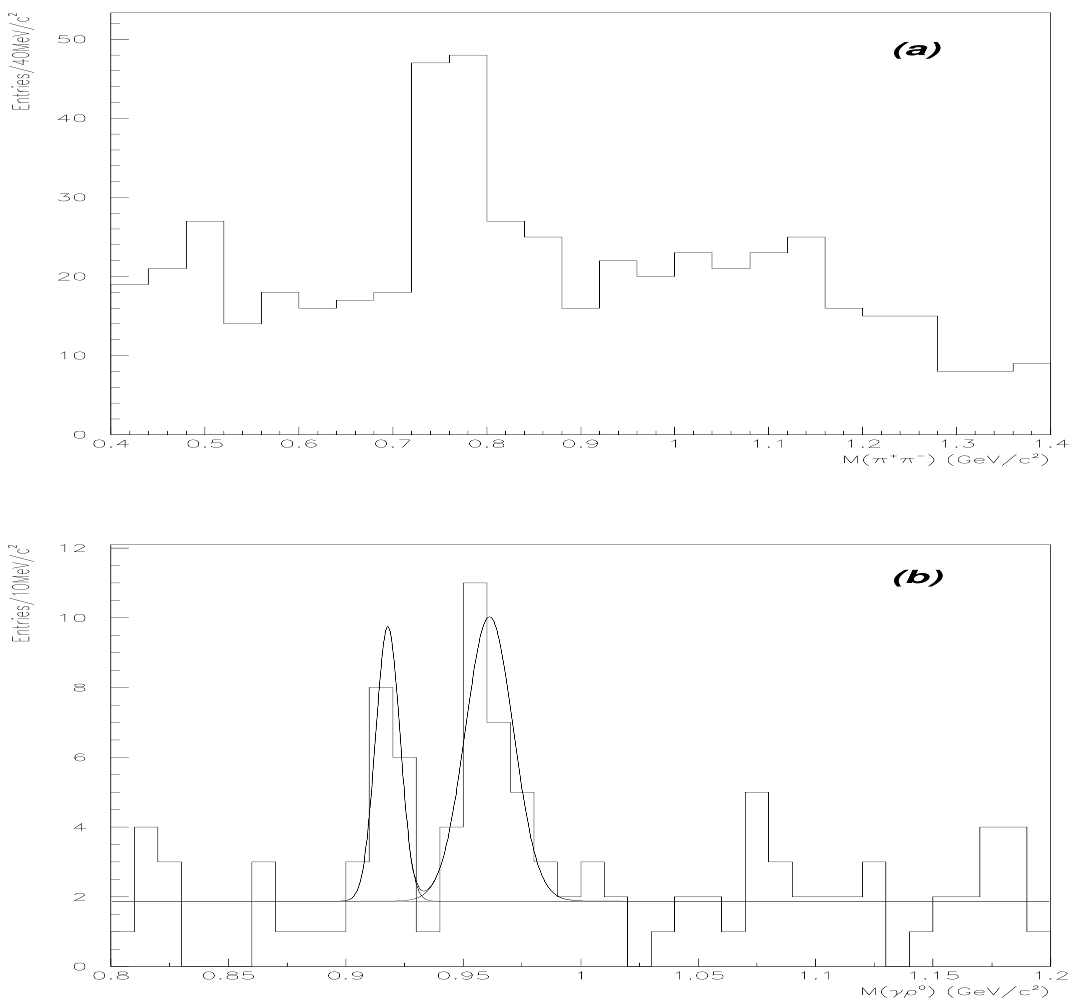

FIG. 2. Invariant mass in $\gamma\gamma\pi^+\pi^-$ final state: (a)$\pi^+\pi^-$, (b)$\gamma\rho^0$.

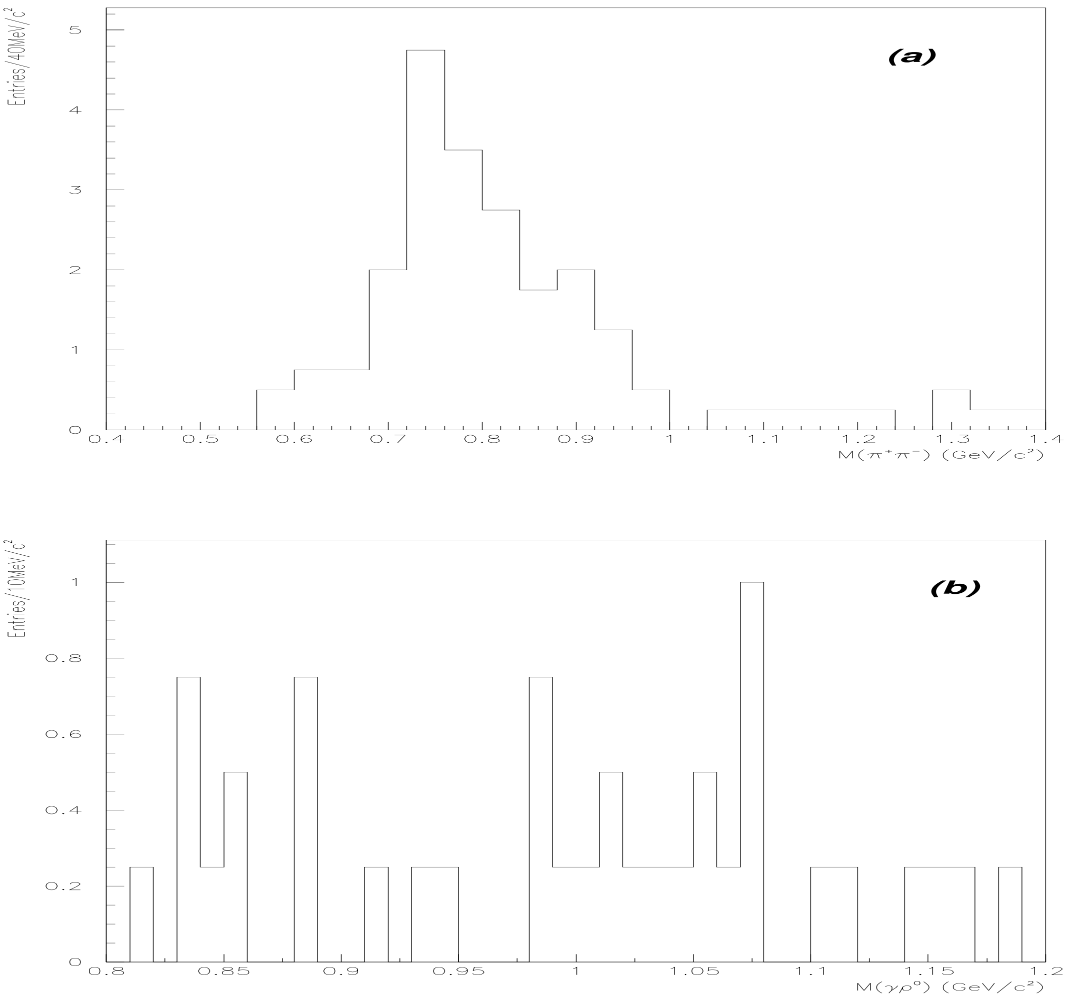

FIG. 3. Background contamination to $\gamma\gamma\pi^+\pi^-$ channel: (a)$\pi^+\pi^-$, (b)$\gamma\rho^0$.